



Earthquake accelerogram denoising by wavelet-based variational mode decomposition

Tara P. Banjade · Siwei Yu  · Jianwei Ma

Received: 14 November 2018 / Accepted: 15 March 2019 / Published online: 8 April 2019
© Springer Nature B.V. 2019

Abstract Earthquake acceleration time chronicles records are important sources of information in the field of tremor engineering and engineering seismology. High frequency noise could considerably reduce P phase picking accuracy and the time. Accurate detection of P phase and onset time arrival picking is very important for the earthquake signal analysis and prediction problem. Large number of those records are defiled with noise so appropriate denoising method is impulse for the exact investigation of the information. Polish off of non-stationary and high energy noise from the recorded signal is challenging with preservation of original features. In this paper, we propose a method to denoise the signal based on variational mode decomposition and continuous wavelet transform. Noisy signal is disintegrated into intrinsic mode function by variational mode decomposition. The probability density function of noisy signal and each intrinsic mode functions is calculated using Kernel density estimation and then Manhattan distance. The probability density function helps us to identify the relevant mode and high frequency noisy intrinsic mode functions, so the continuous wavelet transform is applied to the selected mode. We observed the effect of noise and denoising method on parameters

like acceleration and displacement response spectra. The experiments on synthetic and real earthquake accelerograms validate ameliorate result of the proposed method.

Keywords Earthquake accelerogram · Seismic noise · Continuous wavelet transform · Variational mode decomposition

1 Introduction

Earthquake is an often happening characteristic seismic peril. Generally, the effect of noise in seismic flag is more regrettable at low under 1 Hz and high more than 5 Hz frequencies and signal to noise ratio (SNR) is patently low. Seismic noise can be characterized short and long period caused by natural and artificial sources. Short-term noise by natural sources is broadband, ranging from about 0.5 Hz up to about 15–60 Hz (Young et al. 1996) but the dominant sources of high frequency noises are artificial termed as cultural noise. Natural short period noise couples mostly into surface wave modes, cultural seismic noise, however, couples at least partly into body waves that can propagate also to great depth (Carter et al. 1991). Ground noise at long period 0.2 to 50 mHz are usually associated with pressure and temperature fluctuation and vertical component seismometers react to changes in gravity (Murphy and Savino 1975; Zurn and Wielandt 2007). The information specifically recorded in the

T. P. Banjade · S. Yu (✉) · J. Ma
Department of Mathematics and Artificial Intelligence
Laboratory, Center of Geophysics, Harbin Institute
of Technology, Harbin 150001, China
e-mail: siweiyu@hit.edu.cn

station are mostly sullied with irregular noise which exasperate the seismologist for better and precise count and examination of peak ground acceleration, velocity, displacement, P wave and S wave, etc. Effect of denoising can be realized for accurate detection of P phase and onset time arrival picking, besides this high resolution of the image exposing the hidden important features, detecting small events with preservation, improving signal to noise ratio etc.

Basic architects are relied upon to give more accentuation on outlining structures in light of plan and reaction spectra created from accelerograms which are relied upon to be seismic tremor safe. This is conceivable by the utilization of accelerograms as it gives basic data about the seismic tremor source and is an advantage for the advance in quake what's more, seismological designing. Preparing of the accelerograms is frequently expected to draw out this important data and is regularly not direct because of the nearness of complex attributes like non-stationary and non-linear parts of ground shaking. Also, because of the impact of numerous arbitrary and indeterminate characteristic factors, the watched time arrangement accelerogram information dependably incorporate numerous high recurrence commotions which taint the genuine arrangement information. This causes many difficulties in period identification, parameter estimation, modeling, and system identification. It resembles aphoristic that seismic information are constantly debased by random noise (Chen et al. 2015) in field obtaining which demonstrates the negative effect on the investigation for oil status and other numerous seismic occasions real recognizable proof. Thusly random noise weakening is an exceptionally vital advance for the seismic information handling and planned number of seismic denoising techniques in mathematical and geophysical science. Customary sifting techniques like Wiener filter, Kalman filter, and Fourier strategies were mainstream first and foremost stage; however, these were touchy for linear and stationary signal investigation (Yan et al. 2009). Wavelet is a great degree surely understood procedure for seismic data denoising and besides associated for shudder accelerogram denoising like adjustment of profoundly uproarious solid movement records utilizing a modified wavelet (Ansari et al. 2010; Herranz et al. 2003). The flag of intrigue and the defiled commotion in watched time series information of solid movement accelerograms are accepted to have distinctive variety

characteristics. Hence, the wavelet coefficients portraying the flag of intrigue and clamor are likewise thought to appear as something else (Beena et al. 2012, 2016) P phase picking (Karamzadel et al. 2013) are the some applications of wavelets on earthquake accelerogram denoising.

As a spectral decomposition method, the Empirical Mode Decomposition (EMD) (Huang et al. 1998) has been used in seismic signal processing. Seismic noise can be weakened adequately (Bekara and Baan 2009), EMD to build up a model for portraying slip field on the crack plane (Raghu 2010) and additionally connected as intrinsic mode function (IMF) of quake slip dispersion. Similarly EMD for spectral analysis, random noise attenuation (Han and Baan 2013; Chen et al. 2016) are the few examples of EMD based application on seismic data processing. As of late another great method called synchrosqueezing (SS) (Daubechies et al. 2011) was acquainted deputize EMD. The extensions of EMD, ensemble empirical mode decomposition (EEMD) (Wu and Huang 2009), complete ensemble empirical mode decomposition (CEEMD) (Torres et al. 2011) take care of mode blending issue in some degree.

EMD has number of significant for the seismic information investigation yet amid the procedure of seismic noise lessening. EMD assaults all vitality at high wave number and mode blending issue so it is less successful as far as safeguarding the energy, to right such impediment variational mode decomposition (VMD) is proposed (Dragomiretskiy and Zosso 2014). VMD is considered so obviously better than EMD in various angles like with band confine priority. It accomplishes higher determination in wave number hub while separating the occasions and in denoising every IMFs are kept without disposing of so occasions are better protected and slop protection (Yu and Ma 2017).

In this paper, we propose seismic signal denoising strategy in light of VMD and CWT. VMD method can disintegrate the seismic signal into series of intrinsic mode functions (IMFs) from low to high frequency adaptively. Seismic noise generally appear in the intrinsic mode with high frequencies. So we initially break down the boisterous signal into number of IMFs by VMD then we select some high recurrence mode and significant mode computing the probability density function (PDF) using Kernel density estimation (KDE). The Manhattan distance (MD) between PDF

of boisterous and every IMF is computed which still contain noise and after that relevant IMFs are denoised by CWT technique which guarantees the wiping out of high recurrence solid noise. Subsequently, we can take the benefits of both VMD and CWT technique to improve noise free signal with high SNR with safeguarding the most extreme innovation. We test the proposed system in simple synthetic signal, synthetic and real earthquake accelerogram of Nepal’s seismic tremor 2015.

2 Method

Consider the following equation,

$$x = y + z \tag{1}$$

where x is observed noisy data, y is noise-free data, and z represent the random noise. The approximation is generally done under the presumption that the noise level is cognised. However, in real seismic data the noise level is normally obscure and motive to be estimated from the observed data. Noise level can be estimated based on the principle of minimum statistics (Martin 2001). This approach expect that the signal is more stronger than the clamor; therefore, on the off chance that we track the minima of uproarious power range with a siding window, we will have a gauge relative to the foundation commotion control. We give the quantitative examination of the proposed technique with established strategy Kalman filter and EMD, VMD strategy in SNR by the accompanying equation.

$$SNR = 20 \log_{10} \left(\frac{\|x_0\|_2}{\|x - x_0\|_2} \right)$$

where x_0 is the clean signal and x represents the denoised signal; SNR is measured in dB .

2.1 Similarity measure techniques

Probability density function of a continuous random variable can be deciphered as providing a relative likelihood which is very applicable to measure the similarities (Komaty et al. 2014). To calculate the PDF, we may apply KDE, which is mathematically expressed as,

Let (x_1, x_2, \dots, x_n) be a univariate independent and identically distributed sample drawn from some

distribution with an unknown density f . Then, its kernel density estimator is,

$$\hat{f}_h(x) = \frac{1}{n} \sum_{i=1}^n K_h(x - x_i) = \frac{1}{nh} \sum_{i=1}^n K \left(\frac{x - x_i}{h} \right)$$

where K is the Kernel a non negative capacity that coordinates to one and $h > 0$ is a smoothing parameter called the data transfer capacity. Utilizing this KDE work we compute the PDF of boisterous signal and every IMF which assist us with selecting the applicable modes.

2.2 Continuous wavelet transform

The continuous wavelet transform is executed through a model breaking down capacity known as mother wavelet ψ , which can be rendered as bandpass. The continuous wavelet transform of any signal $x(t)$ at scale a and time shift τ is given by Daubechies and Heil (1992)

$$W_x(a, \tau) = \langle x, \psi_{a,\tau} \rangle = \int_{-\infty}^{+\infty} x(t) a^{-\frac{1}{2}} \psi^* \left(\frac{t - \tau}{a} \right) dt. \tag{2}$$

where $*$ denotes the complex conjugate, $\langle x, \psi \rangle$ is the inner product and W_x is the coefficient representing to the limited vitality of the signal x in the concentrated time recurrence picture. The mother wavelet ψ must be square integrable capacity, where its Fourier transform $\hat{\psi}(\zeta)$, ought to vanish at zero frequency. The real contrast between CWT and discrete wavelet transform (DWT) is the manner by which the scale parameter is discretize. The CWT discretize scale more finely than DWT. The discretized wavelets for CWT is

$$\frac{1}{\sqrt{2^j/v}} \psi \left(\frac{n - m}{2^j/v} \right)$$

where v is an integer greater than 1 and $j = 1, 2, 3, \dots$

Also discretized wavelet for DWT is,

$$\frac{1}{\sqrt{2^j}} \psi \left(\frac{n - m}{2^j} \right).$$

To denoise the signal by DWT method, we must select the reasonable thresholds may be soft or hard. Yet, we can decipher the CWT as a recurrence-based

bandpass filtering of the signal by changing the CWT as a inverse Fourier transform

$$C(a, b; f(t), \psi(t)) = \frac{1}{2\pi} \int_{-\infty}^{\infty} \hat{f}(w)\hat{\psi}(aw)e^{iwb}dw \tag{3}$$

where $\hat{f}(w)$ and $\hat{\psi}(w)$ are the Fourier transform of the signal and wavelet (Daubechies and Heil 1992).

2.2.1 Variational mode decomposition

Variational mode decomposition is planned to break down a composite signal into an ensemble of band-limited modes termed IMFs, which are portrayed by the sparsity in the bandwidth which is gotten by solving an optimization problem (Dragomiretskiy and Zosso 2014)

$$\min_{\{u_k\}\{\omega_k\}} \left\{ \sum_k \|\partial_t \left[\left(\delta(t) + \frac{j}{\pi t} \right) u_k(t) \right] e^{-j\omega_k t} \|_2^2 \right\} \tag{4}$$

such that

$$\sum_k u_k = f$$

where u_k is the k th disintegrated mode of the signal, $\{u_k\}$ refers an ensemble of modes $\{u_1, u_2, \dots, u_k\}$, w_k is the center frequency of the corresponding k th mode of the signal, $\{w_k\}$ is an ensemble of center frequencies related to the modes after disintegration $\{w_1, w_2, \dots, w_k\}$, $f(t)$ is the input signal and $\delta(t)$ is the Dirac function. Additionally, the verbalization $\left(\delta(t) + \frac{j}{\pi t} \right) * u_k(t)$ is the Hilbert transform of $u_k(t)$, which goes for changing $u_k(t)$ into the logical signal remembering the true objective to make an uneven repeat run with simply positive frequencies. The exponential term $e^{-j\omega_k t}$ makes the recurrence range of every mode move to the baseband. Besides, the data transmission of every mode dictated by squared standard of the inclination (Dragomiretskiy and Zosso 2014). The alternating direction method of multipliers (ADMM) approach can be applied to solve Eq. 4, which delivers an outfit of mode parts and the relating focus recurrence. Every mode evaluated from arrangements in the recurrence area is spoken to as:

$$\hat{u}_k^{n+1}(w) = \frac{f(\hat{w}) - \sum_{i=1}^{k-1} \hat{u}_i^{n+1}(w) - \sum_{i=k+1}^K \hat{u}_i^n(w) + \frac{\hat{\lambda}^n(w)}{2}}{1 + 2\alpha(w - w_k^n)^2} \tag{5}$$

$$w_k^{n+1} = \frac{\int_0^\infty w |\hat{u}_k^{n+1}(w)|^2 dw}{\int_0^\infty |\hat{u}_k^{n+1}(w)|^2 dw} \tag{6}$$

where $\hat{f}(w)$, $\hat{u}_i(w)$, $\hat{\lambda}(w)$, and $u_k^{n+1}(w)$ represent the Fourier transforms of $f(t)$, $u_i(t)$, $\lambda(t)$ and $u_k^{n+1}(t)$, respectively, and n is iterations (Liu et al. 2017; Dragomiretskiy and Zosso 2014). It can be watched that Eq. 5 is recognized as a Wiener filtering system, which specifically refreshes the mode in Fourier space. What’s more, we can extricate the genuine part for the opposite Fourier transform of the proposed expository signal with a specific end goal to acquire these modes after decay in the time domain. Then again, the middle recurrence of the evaluated mode w_k^{n+1} can be effectively gotten by Eq. 6, which puts the new focus recurrence at the focal point of the gravity of the related mode’s capacity range.

The VMD method disintegrate the seismic signal $x(t)$ into low to high frequencies, which can be explained as (Liu et al. 2017)

$$f(t) = \sum_{i=1}^N u_i(t)$$

where $f(t)$, $u_i(t)$ represent the observed signal and the i th IMF, respectively, and N represent number of IMF. So we can make characterization IMF in noise overwhelming and noise prevailing as

$$f(t) = \sum_{i=1}^M u_i^{noise}(t) + \sum_{i=M+1}^N u_i^{signal}(t)$$

where $u_i^{noise}(t)$, $u_i^{signal}(t)$ are the noise prevail modes and signal prevail modes respectively, and M represents the division between noise and signal (Liu et al. 2017). As the VMD strategy can break down the seismic flag into arrangement of inborn modes from low recurrence to high recurrence adaptively. Seismic noise for the most part show up in the characteristic mode with high frequencies.

2.2.2 VMD-CWT method

We now select the noise prevailing modes and allow them to be further denoising. For the selected high frequency IMF, we apply CWT and inverse continuous

wavelet transform (ICWT) to reproduce the signal. The term $W_x(a, \tau)$ in CWT should be evacuated to make the division administrator numerically stable and CWT can be connected as bandpass filtering strategy as

$$w(F, t) = \begin{cases} 0 & \text{for, } F > F_2 \\ 0 & \text{for, } F < F_1 \\ w(F, t) & F_1 \leq F \leq F_2. \end{cases}$$

The scale α and frequency F are in contrarily corresponding connection, w speaks to the CWT coefficients F_1 and F_2 represents upper and lower frequencies. F is the coveted stop-band weakening in dB, take note of that this gauge for w turns out to be too little when the channel pass-band width approaches zero. We set F_1, F_2 on chose IMFs keeping on mind that concentrate the commotion and protect inventiveness with number of examination. The CWT registers the internal result of the signal $x(t)$, with interpreted and enlarged adaptations of investigating wavelet $\psi(t)$. We can see that extending a wavelet in time makes its help in the recurrence space recoil. Notwithstanding contracting the recurrence bolster, the inside recurrence of the wavelet shifts toward bring down frequencies. This portrays the CWT as a bandpass filtering of the input signal. CWT coefficients at bring down scales speak to vitality in the info motion at higher frequencies, while CWT coefficients at higher scales speak to vitality in the information motion at bring down frequencies. Notwithstanding, not at all like Fourier bandpass sifting the width of the CWT channels diminishes with expanding scale. In the wavelet change, the scale or widening activity is characterized to safeguard vitality. To save vitality while contracting the recurrence bolster necessitates that the pinnacle vitality level increments. With these properties of CWT, here, we apply for selected high frequency IMFs and we add all IMFs including low frequency to reconstruct the denoised result which ensures the more noise free signal with increment of SNR.

3 Results and discussion

3.1 Similarities measure test

Probability density function of a continuous random variable can be interpreted as providing a relative

likelihood which is very applicable to measure the similarities. To calculate the PDF, we use the Kernel density estimation function of noisy signal and each IMFs. From above Fig. 1, we see the PDF of IMF 1, IMF 2, IMF 3 IMF 4 are in a same pattern and are relevant. This implies that these IMFs are compose of low frequency, but the PDF plot of noisy and IMF 5 are in comparatively close pattern so IMF 5 consists of high frequency noise. Also we calculate the Manhattan distance of PDF between noisy and each IMF. By identifying the high frequency noisy IMF, we further introduce CWT method and reconstruct the signal.

3.2 Synthetic data test

To approve the techniques, we first test on synthetic seismogram signal as appeared in Fig. 2. We include arbitrary noise with SNR 5 dB and apply distinctive denoising strategies, it is watched that the proposed technique produce the relatively more smooth signal with higher SNR and ready to recoup the nearby comparable unique signal from the ruined one. The numerical information clarifies that for SNR esteem given by Kalman, EMD, VMD and proposed strategy are 8 dB, 10 dB, 13 dB, and 15 dB individually as specified in Table 1. When we denoise by Kalman filter it is not delicate for the non stationary signal for EMD process we evacuate first IMF in which there is high probability of losing the data on first IMF. So we apply VMD technique to break down into number of IMF where VMD decay the signal from low recurrence to high recurrence, we watched that some high recurrence IMF still contains the commotion so we additionally apply continuous wavelet transform on chosen IMF to guarantee the more noise free signal with better conservation of the inventiveness. During the denoising processing, minimizing phase shift is one of the challenging problem, as big phase shift disturb wave arrival time which leads all the analysis less accuracy. Here, we found that our method arise small phase shift. The signal denoised by Kalman filter has big phase shift Fig. 2c and by other methods like EMD Fig. 2d, VMD Fig. 2e also appear but it is minimizes in the proposed method Fig. 2f. VMD is recently developed adaptive signal decomposition method and an adaptive for non stationary signal solving the mode mixing problem and non optimal reconstruction problem. As our method based on these, it can minimizes the such limitations.

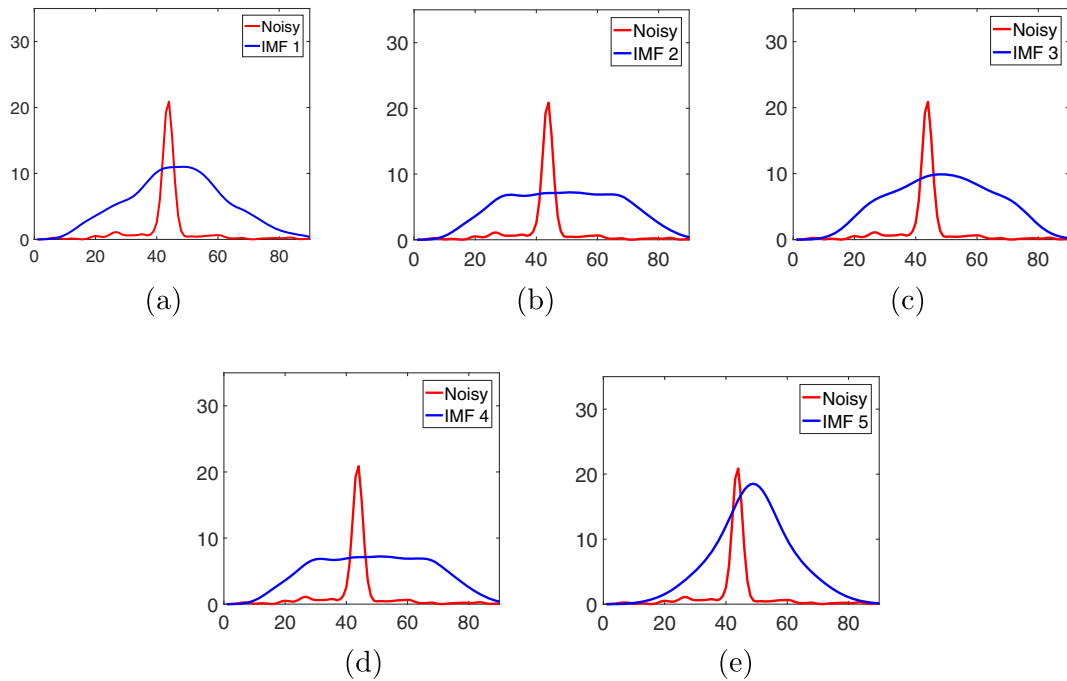


Fig. 1 Probability density function of noisy signal and **a** IMF 1, MD = 218 **b** IMF 2, MD = 247 **c** IMF 3, MD = 220 **d** IMF 4, MD = 228 **e** IMF 5, MD = 179

Next we choose the synthetic earthquake accelerogram as in Fig. 3 to observe the effect of noise on peak ground acceleration, velocity, and displacement

component. This synthetic signal is designated as frequency vector containing 2048 points, taking bandwidth of the earthquake excitation 0.3, standard

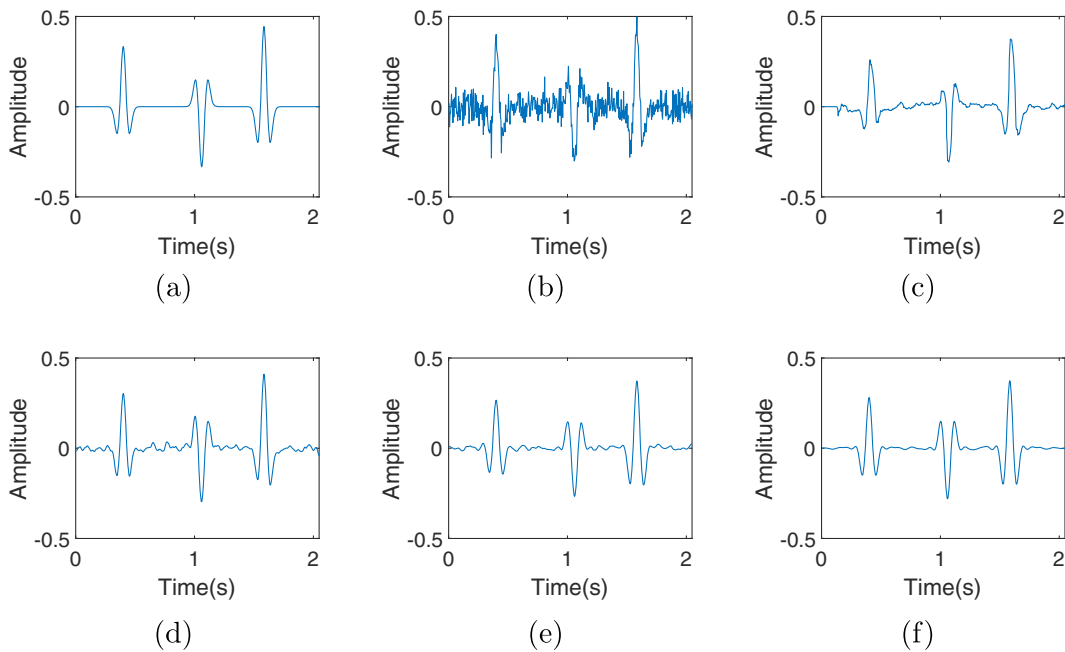


Fig. 2 Synthetic data test. **a** Original signal. **b** Noisy signal with SNR = 5 dB. **c** Denoised by Kalman filter, SNR=8 dB. **d** By EMD, SNR=10 dB. **e** By VMD, SNR=13 dB. **f** By the proposed method, SNR = 15 dB

Table 1 SNR values of four different methods applied to the synthetic data in Fig. 2 with different relative percentage of noises

Noise variances	0.01	0.25	0.5	0.75
Input noisy data	10	7	5	2
Kalman	14	10	8	5
EMD	14.5	14	10	7
VMD	15	14	13	9
Proposed	17	16	15	10

deviation of the excitation 0.3, dominant frequency of the earthquake excitation 5 Hz, value of the envelope function at ninety percent of duration 0.2, normalized duration time when ground motion achieves peak 0.4, duration of ground motion 20 second. The time series is generated in two steps, first a stationary is created based on the Kanai-Tajimi spectrum (Guo and Kareem 2016) then envelope function is used to transform this stationary time series into a non stationary record (Rofooei et al. 2001). The velocity component can be obtained simply integration on acceleration

with respect to time and displacement component can be obtained by integration on velocity with respect to time as,

$$v = \int a dt, d = \int v dt$$

where a , v , and d are acceleration, velocity, and displacement respectively.

As we realize that displacement is the fundamental constituent for the accelerogram, we have to concern how the impact fall on the essential constituent amid the seismic information preparing. Peak ground acceleration (PGA), velocity (PGV), and displacement (PGD) are the most critical parameter on tremor seismology in light of this parameter designers can examine the idea of soil on the specific territory and can prescribe the reasonableness to develop the structures and other physical foundation that may safe amid the quake debacle.

The peak ground displacement esteem gives the position change of the earth surface and shaking degree. By investigating the vertical segment and horizontal segment, we can affirm the idea of earth’s

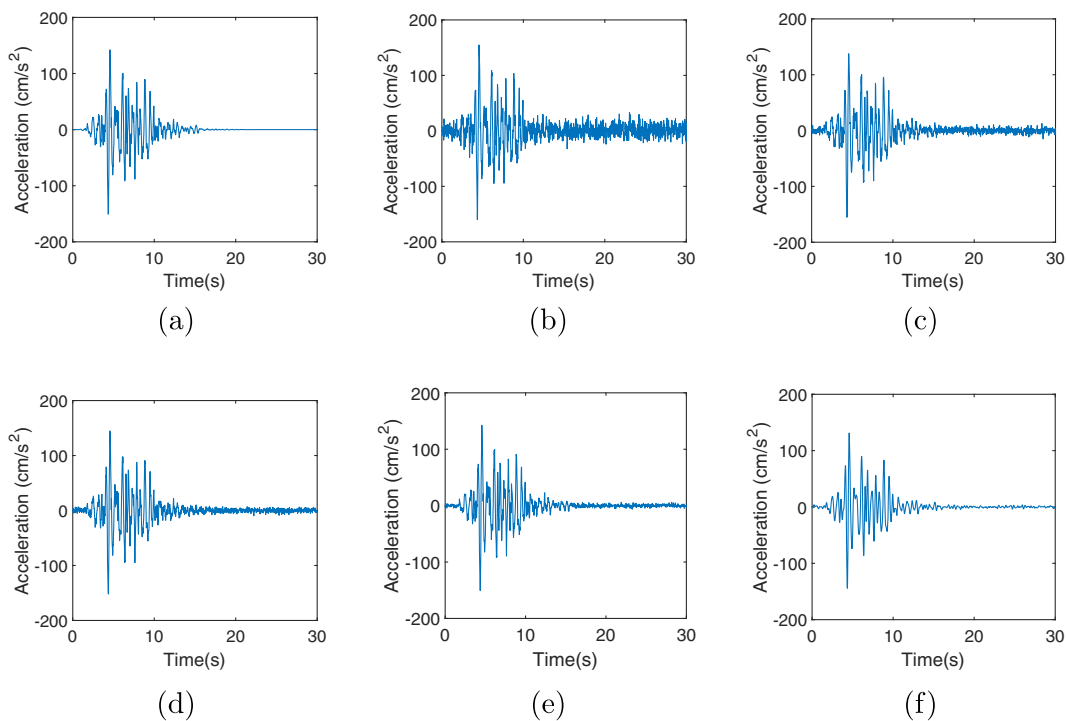


Fig. 3 Effect of noise in synthetic earthquake accelerogram max. value and SNR test. **a** Original signal. **b** Noisy signal with SNR = 5 dB. **c** Denoised by Kalman filter, SNR=9 dB. **d** By

EMD, SNR=10 dB. **e** By VMD, SNR=11 dB. **f** By the proposed method, SNR = 12 dB

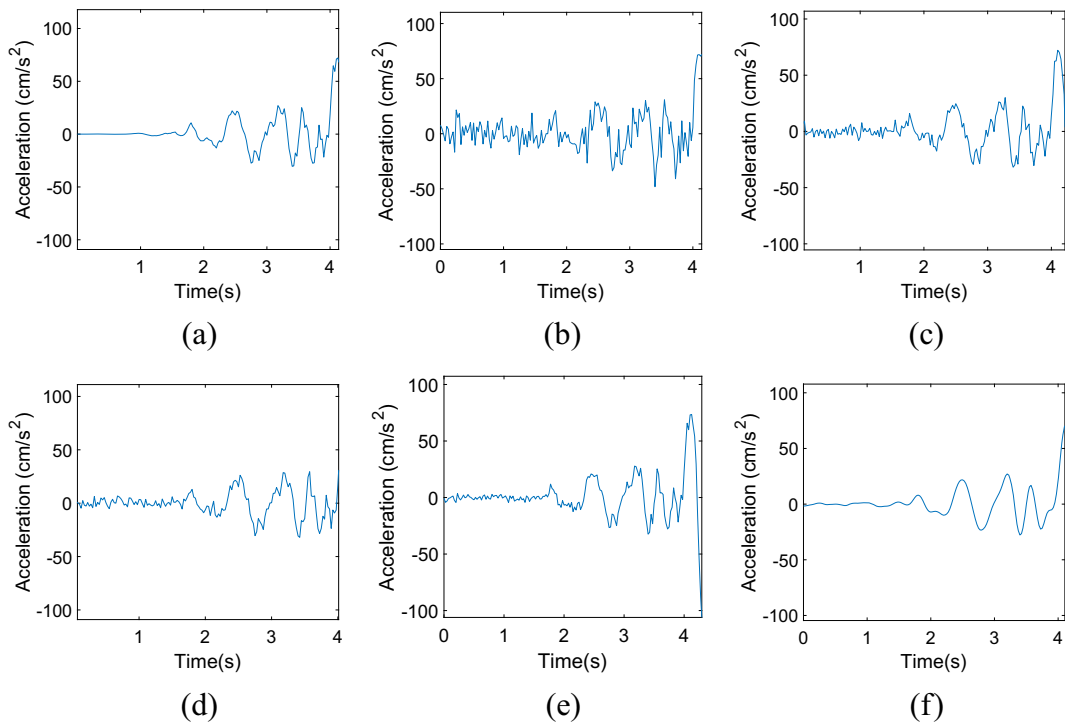


Fig. 4 Zoom version of synthetic earthquake accelerogram data test. **a** Original signal. **b** Noisy signal. **c–f** Denoised by Kalman filter, EMD, VMD, and the proposed method

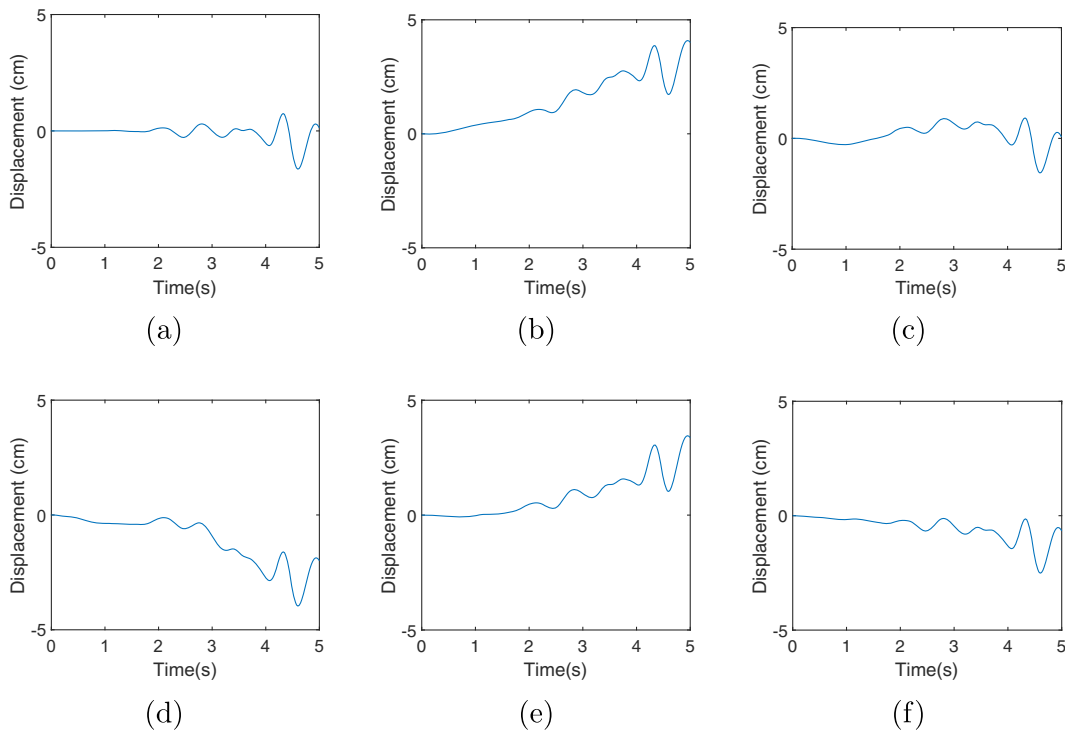


Fig. 5 Displacement component with noise effect and max.value derived from synthetic accelerogram. **a** Original signal. **b** Noisy signal. **c–f** Denoised by Kalman filter, EMD, VMD, and the proposed method

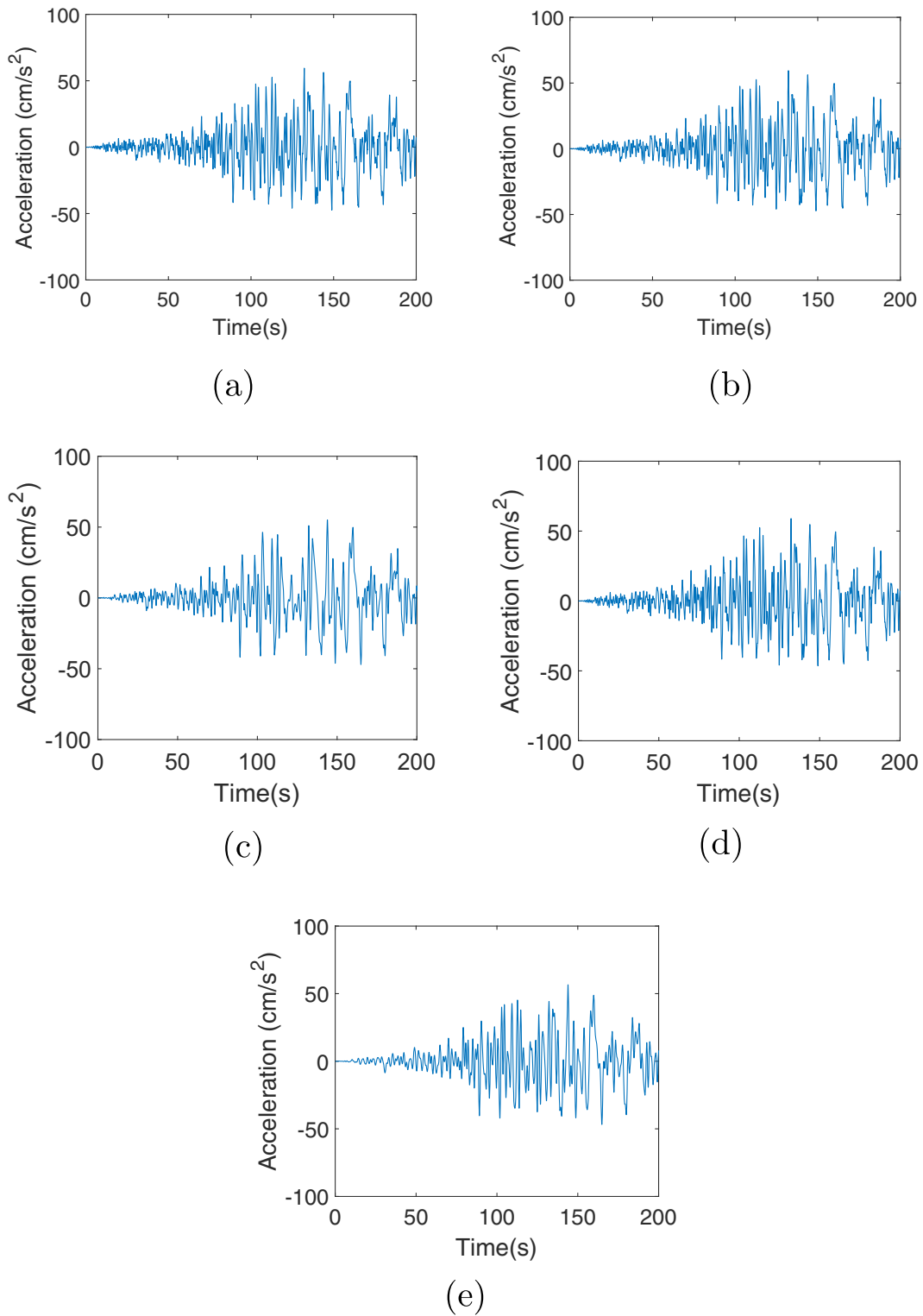


Fig. 6 Effect of noise on real earthquake accelerogram with max. value test. **a** Noisy signal. **b–e** Denoised by Kalman filter, EMD, VMD, and the proposed method

development and the specific soil structure. We test the impact of clamor on peak ground acceleration and displacement. From Fig. 3, we found PGA of noise free signal accelerogram is 150 cm/sec^2 but when we add some random noise its value found 168 cm/sec^2 . Also for PGD value for original synthetic signal is 2.3 cm but for noisy signal is 4.1 cm, this implies that parameters like PGA and PGD vary according to the noise presence. At the mean time, we apply different denoising methods for the noise accelerogram and got the

PGA value as 143 cm/sec^2 , 167 cm/sec^2 , 155 cm/sec^2 , and 152 cm/sec^2 for Kalman, EMD, VMD and proposed methods. Figure 4 expose the zoom version of the Fig. 3 that indicates the smoothness of the region for P phase arrival point.

Also PGD is obtained as 1.7 cm, 4.3 cm, 3.7 cm, and 2.8 cm for Kalman, EMD, VMD, and proposed methods respectively. Based on this result, we can conclude that Kalman and EMD method can denoise the signal but they harm for inaccurate calculation for

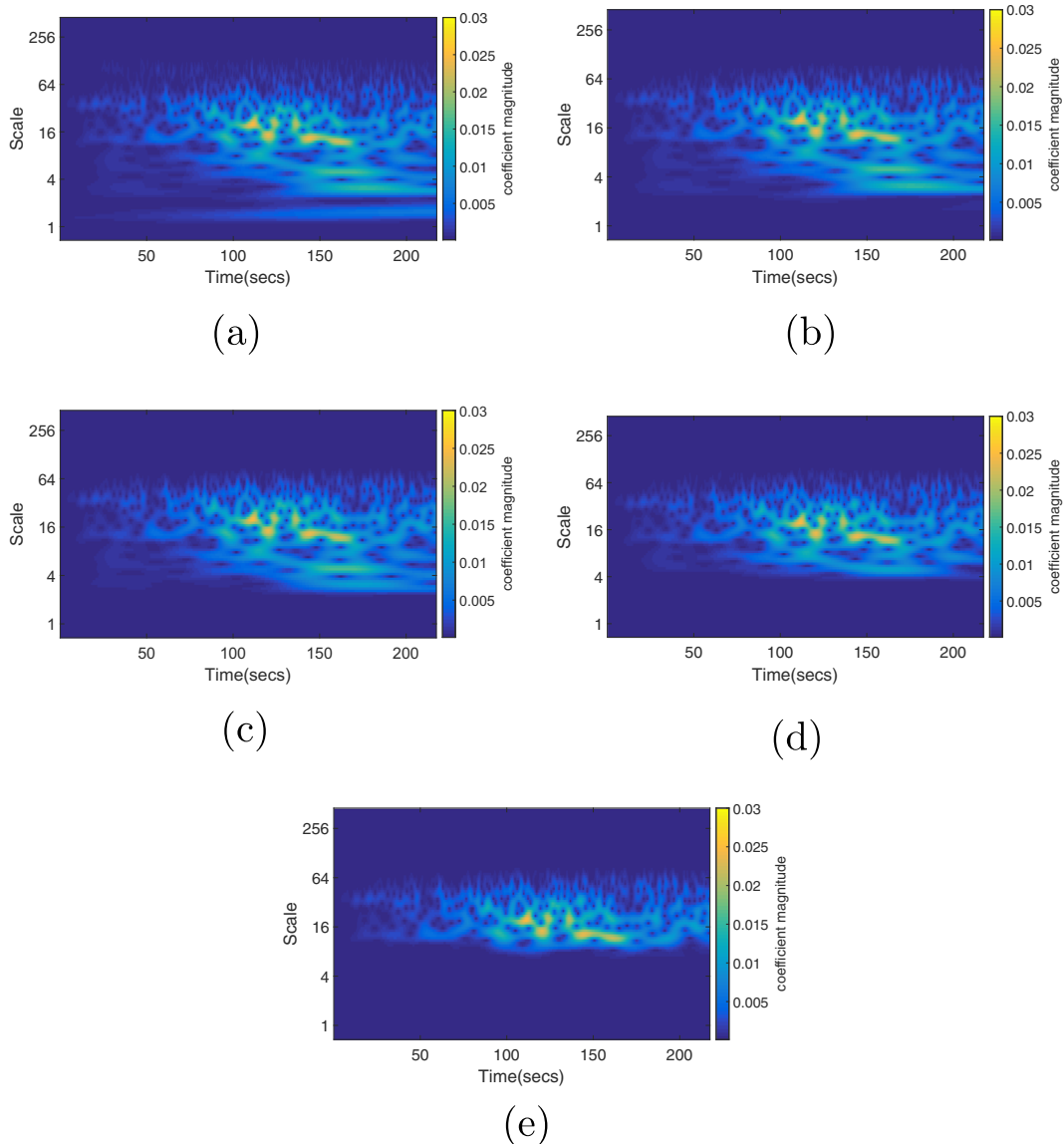


Fig. 7 Corresponding Scalogram for real earthquake data of Fig. 6. **a** Noisy signal. **b–e** Denoised by Kalman filter, EMD, VMD, and the proposed method

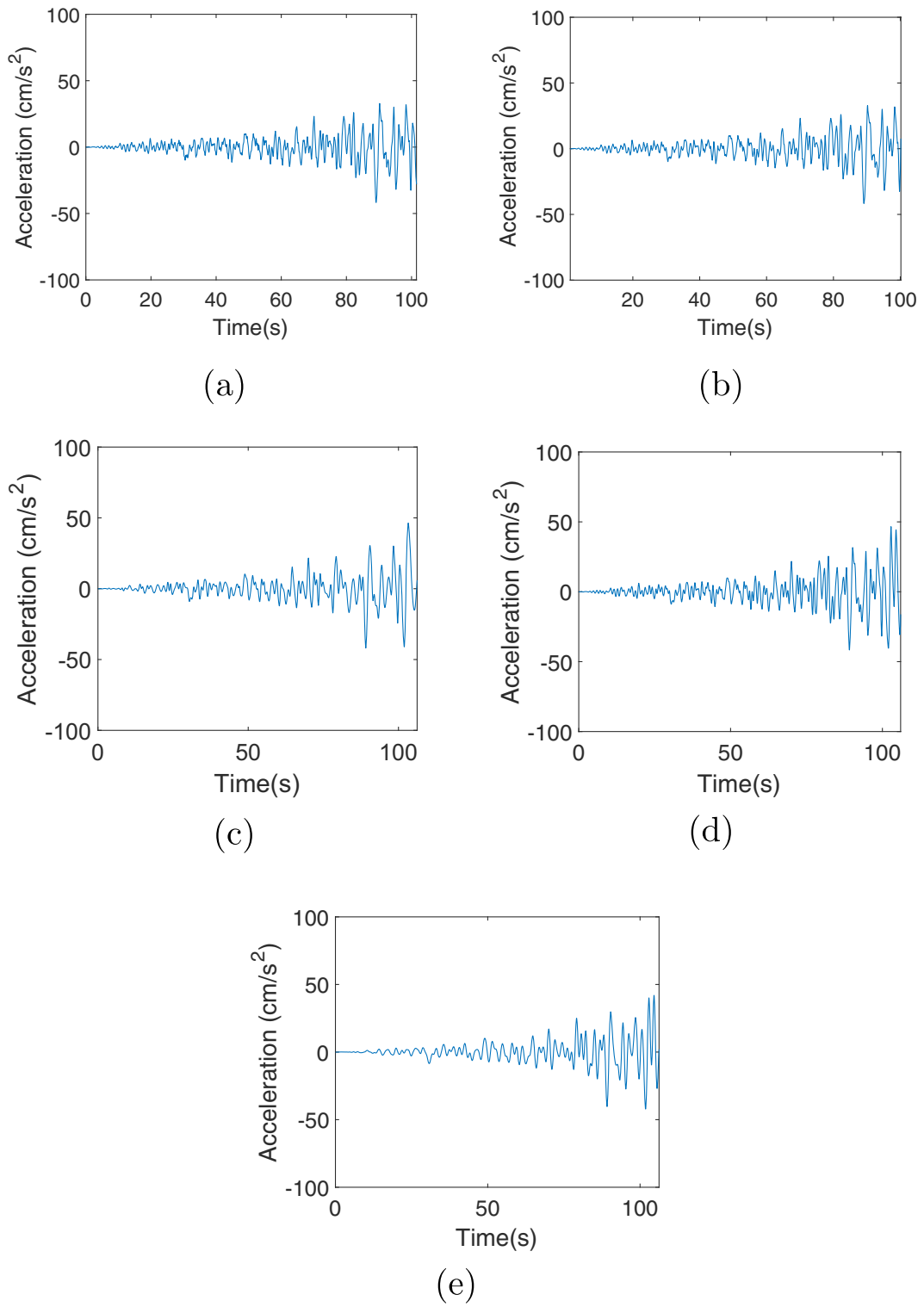


Fig. 8 Zoom version of real earthquake accelerogram data test. **a** Noisy signal. **b–e** Denoised by Kalman filter, EMD, VMD, and the proposed method

PGA and PGD as its more deviation from original signal but VMD and proposed methods can give better denoised result with close PGA and PGD value with original signal.

Here, we observed that during the denoising by different process the peak ground displacement varies with the noise on synthetic earthquake records. The Kalman filter and EMD can give the denoised result

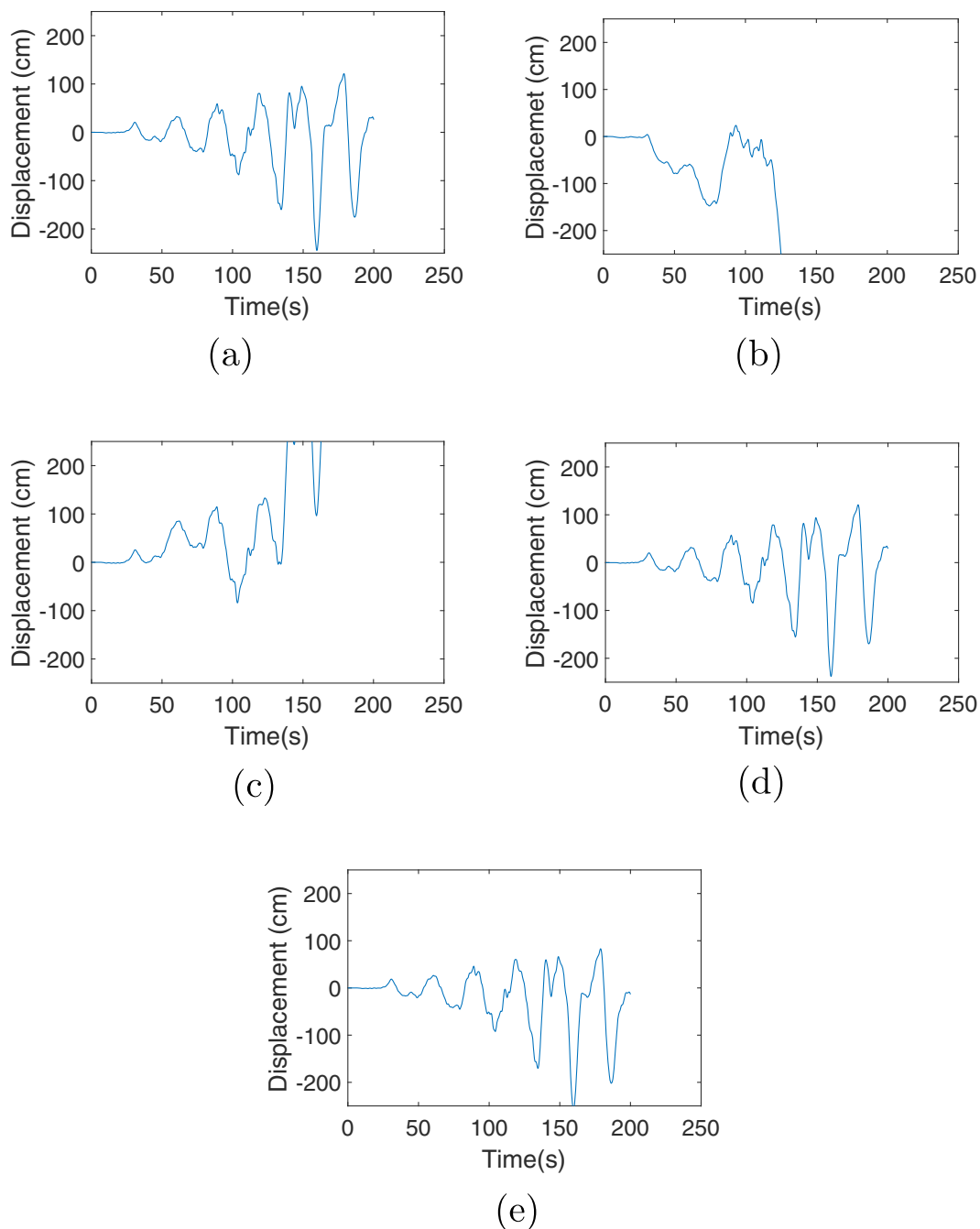


Fig. 9 Displacement component with noise effect and max. value derived from real earthquake accelerogram data test. **a** Noisy signal. **b–e** Denoised by Kalman filter, EMD, VMD, and the proposed method

but they are not stable for the displacement coefficient as in Fig. 5.

3.3 Real earthquake data test

At last, we applied methods on real earthquake accelerogram which was recorded in the Department of Mine and Geology, Nepal during Nepal’s earthquake in April 2015 with magnitude 7.8.

For real earthquake accelerogram signal, the peak ground acceleration of the data which we use is 59 cm/sec² which is supposed to contain the noise. After denoising by Kalman, EMD, VMD, and by proposed method, PGA value was noticed as 56 cm/sec², 55 cm/sec², 57 cm/sec², and 58 cm/sec² respectively. The corresponding scalogram plot of the real earthquake accelerogram of Fig. 6 is shown in Fig. 7 which displays the wavelet scale as a function of time. Color intensity at any point in the picture corresponds to the coefficient magnitude of a wavelet with a particular period at a particular point of the time series. Figure 7e shows the proposed method successfully removed the noise with preserving the feature and strong energy section compare to the other existing methods. It can simultaneously achieve accurate frequency representation for low frequencies, and good time resolution for high frequencies.

The effect of denoising on the synthetic and real earthquake data has been observed very clearly based on the tool which we used to denoise the seismic signal. In Fig. 9, the displacement coefficient that obtained from noisy real earthquake accelerogram whose maximum value is 244 cm and after the denoising by Kalman, EMD, VMD and proposed method got 528 cm, 582 cm, 237 cm and 250 cm respectively as mentioned in Table 3. Figure 8 represents the zoomed version of Fig. 6 that show the P phase region of the signal. Based on this we can conclude that traditional methods like Kalman and EMD are not sensitive during the denoising process as there is great deviation on original displacement coefficient and VMD and the proposed method denoise the signal very well with high SNR and does not allow to deviate the displacement component with compare to the original one.

These parameters like peak ground acceleration, velocity and displacement have an exceptionally hugeness in quake building so amid the denoising procedure we should concern to take the precise estimation

Table 2 SNR (in dB) result for synthetic accelerogram test

Data/Method	Noisy	Kalman	EMD	VMD	Proposed
Synthetic earthquake accelerogram	5	9	10	11	12

of these parameter. On the off chance that we apply conventional strategy to denoise the signal yet comprehend essential constituent displacement which leads for erroneous figuring of PGA, PGV, and PGD (Fig. 9).

The detail result on peak ground acceleration, (cm/sec²) and peak ground displacement (cm) is given in Table 2.

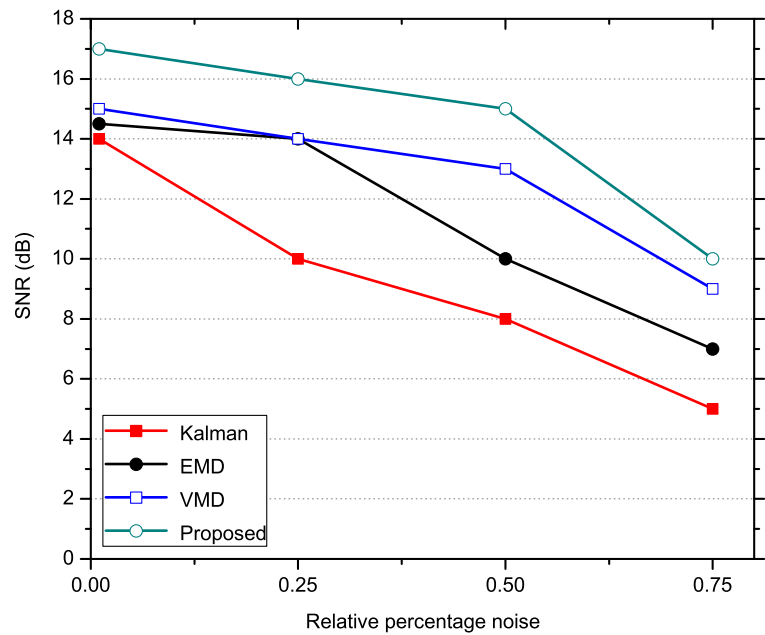
At last, we give a few discourses on velocity and displacement segments. We denoise the seismic tremor accelerogram signal which speak to the ground acceleration, mathematically by integration on acceleration with respect to time we can get velocity and integration on velocity we get displacement. This implies that displacement is the basic constituent of the acceleration. During the denoising on accelerogram signal, we unmistakably watched that clamor is expelled altogether with change on SNR. The impact of various denoising techniques are seen as looking at the peak ground acceleration an incentive from both synthetic and real tremor accelerogram that demonstrates the both commotion expel and protecting about the same PGA and PGD esteems by the proposed strategy.

For the velocity and displacement part, we found that the impact and nearness of clamor can not watched altogether but rather essentially. We can watch the peak ground velocity and displacement esteem which show the techniques by which we denoise the signal that can bode well for exact estimation synthetic accelerogram PGD. As in Table 3, the PGD esteem for synthetic accelerogram of unique is 2.3 cm, denoised by Kalman 1.7 cm, by EMD 4.3 cm,

Table 3 PGA and PGD result for synthetic earthquake accelerogram different test

Method	Original	Noisy	Kalman	EMD	VMD	Proposed
PGA (cm/sec ²)	150	168	143	167	155	152
PGD (cm)	2.3	4.1	1.7	4.3	3.7	2.8

Fig. 10 Performance plots (SNR values) of different methods applied to synthetic data in Fig. 2 and Table 1 with different relative percentage of noises



by VMD 3.7 cm and by proposed technique is 2.8 cm this additionally confirm PGD estimation of unique and in the wake of denoising by proposed strategy demonstrates closeness.

This impact is altogether reside in real earthquake accelerogram. The PGA and PGD esteems given by original signal and denoised by proposed strategy give the more comparable qualities than other technique. Kalman filter and EMD technique can denoise the signal however they vicious the essential constituent displacement segment by veering off with expansive scale with contrast with unique one. This makes the issue to ascertain the exact PGA and PGD esteems. However, in the event that we pick a reasonable denoising strategy like the proposed one, it does not make more contrasts on these parameters. We have used amplitude of all sampling point for comprison in the synthetic test, since SNR is computed with all values. In terms of SNR, it also achieves higher values than the other three methods in all noise levels as indicated in Tables 1 and 2 and Fig. 10. To calculate

the SNR values for all sampling point in real data is complicated as the degree of real noise is unknown (Table 4).

4 Conclusion

We have actualized a seismic denoising enhanced technique in view of VMD algorithm. We observed that there is an impact of noise and denoising strategy on quake accelerogram signal. The proposed strategy gives more critical outcome than conventional technique and EMD; exceptionally, this technique is extremely huge on quake accelerogram denoising. We watched that the clamor nearness on the accelerogram influences the incorrect count on PGA and PGD and diverse techniques to give the distinctive digressed estimation of these parameters. In view of the PGD esteem earthquake engineers can investigate the idea of soil to suggest foundation development in a specific district, this technique is exceptionally touchy one might say of to precise count of some parameter like peak ground acceleration, velocity, and displacement and to watch the impact of noise and the impact of various denoising strategy in these parameters. Accurate detection of P phase and onset time arrival is very important for the earthquake signal analysis and prediction problem, so the dealing with noise

Table 4 PGA and PGD result for real earthquake different test

Method	Original	Kalman	EMD	VMD	Proposed
PGA (cm/sec ²)	59	56	55	57	58
PGD (cm)	244	528	582	237	250

with appropriate denoising method is very important. Here, we applied wavelet-based VMD technique to get noise-free signal with safeguarding of original features.

Acknowledgments The authors would like to thank the Department of Mine and Geology, Nepal, for providing the real earthquake accelerogram data, and thank to Wenlong Wang and Yuhang Shui for the helpful discussions.

Funding information This study is supported in part by National Key Research and Development Program of China under Grant 2017YFB0202900, NSFC under Grant 41625017 and 41804102.

References

- Ansari A, Noorzad A, Zafarani A, Hessam V (2010) Correction of highly noisy strong motion records using a modified wavelet de-noising method. *Soil Dyn Earthq Eng*: 1168–1181
- Beena M, Prabavathy S, Mohanalin J (2012) Wavelet based seismic signal de-noising using Shannon and Tsallis entropy. *Computers and Mathematics with Applications* 64:3580–3593
- Beena M, Mohanalin J, Prabavathy S, Jordina T (2016) A novel wavelet seismic denoising method using type II fuzzy. *Appl Soft Comput* 48:507–521
- Bekara M, Baan M (2009) Random and coherent noise attenuation by empirical mode decomposition. *Geophysics* 74(5):89–98
- Carter JA, Barstow N, Pomeroy PW, Chael EP, Leahy PJ (1991) High frequency seismic noise as a function of depth. *Bull Seismol Soc Am* 81(4):1101–1114
- Chen Y, Ma J, Fomel S (2016) Double-sparsity dictionary for seismic noise attenuation. *Geophysics* 81(2):17–30
- Chen Y, Gan D, Liu T, Yuan J, Zhang Y, Jin Z (2015) Random noise attenuation by a selective hybrid approach using empirical mode decomposition. *J Geophys Eng* 12: 12–25
- Daubechies I, Heil C (1992) Ten lectures on wavelets. *Computers in physics: AIP Publishing*
- Daubechies I, Lu J, Hau T (2011) Synchrosqueezed wavelet transforms: an empirical mode decomposition-like tool. *Appl Comput Harmon Anal* 30:243–261
- Dragomiretskiy K, Zosso D (2014) Variational mode decomposition. *IEEE Trans Signal Process* 62(3):531–544
- Han J, Baan M (2013) Empirical mode decomposition for seismic time-frequency analysis. *Geophysics* 78(2):9–19
- Huang N, Shen Z, Long S, Wu M, Shih H, Zheng Q, Yen N, Tung C, Liu H (1998) The empirical mode decomposition and the Hilbert spectrum for nonlinear and non-stationary time series analysis. *Proceedings The Royal Society* 454(1971)
- Herranz J, Sergio M, Botella F (2003) De-noising of short-period seismograms by wavelet packet transform. *Bull Seismol Soc Am* 93(6):2554–2562
- Karamzadel N, Doloei G, Reza A (2013) Automatic earthquake signal onset picking based on the continuous wavelet transform. *IEEE Trans Geosci Remote Sens* 51(5):2666–2674
- Komaty A, Boudraa AQ, Augier B, Dare-Emzivat D (2014) EMD Based filtering using similarity measure between probability density functions of IMFs. *IEEE Transactions on Instrumentation and Measurement* 63:27–34
- Guo Y, Kareem A (2016) Generation of artificial earthquake records with a non stationary Kanai - Tajimi model. *Eng Struct* 23(7):827–837
- Liu W, Cao S, Wang Z (2017) Application of variational mode decomposition to seismic random noise reduction. *J. Geophys Eng* 14(4):888–899
- Martin R (2001) Noise power spectral density estimation based on optimal smoothing and minimum statistics. *IEEE Transactions on Speech and Audio Processing* 9:504–512
- Murphy AJ, Savino JR (1975) A comprehensive study of long period (20–200 s) Earth noise at the high gain worldwide seismograph stations. *Bull Seismol Soc Am* 65:1827–1862
- Raghu K (2010) Intrinsic mode function of earthquake slip distribution. *World Scientific. Adv Adapt Data Anal* 2:193–215
- Rofooei FR, Aghababaii M, Ahmadi G (2001) Generation of artificial earthquake records with a nonstationary Kanai-Tajimi model. *Eng Struct* 23, 7:827–837
- Torres M, Colominas M, Schlotthauer G, Flandrin P (2011) A complete ensemble empirical mode decomposition with adaptive noise. In: *IEEE international conference on acoustic speech and signal processing*, pp 4144–4147
- Wu Z, Huang N (2009) Ensemble empirical mode decomposition: a noise-assisted data analysis method. *Adv Adapt Data Anal* 1(1):1–49
- Yan F, Dong W, Ji W, Qing P, Zhu L (2009) Entropy-based wavelet de-noising method for time series analysis. *Entropy* 11:1123–1147
- Young ChJ, Chael EP, Withers MW, Aster RC (1996) A comparison of the high-frequency (> 1 Hz) surface and subsurface noise environment at three sites in the United States. *Bull Seism Soc Am* 86, 5:1516–1528
- Yu S, Ma J (2017) Complex variational mode decomposition for slop preserving denoising. *IEEE Trans Geosci Remote Sens* 99:1–12
- Zurn W, Wielandt E (2007) On the minimum of vertical seismic noise near 3 mHz. *Geophys J Int* 168:647–658

Publisher's note Springer Nature remains neutral with regard to jurisdictional claims in published maps and institutional affiliations.